DNA damage-induced ubiquitylation:emerging regulators enforce protective mechanisms

Typas, D.

5

The E3 ubiquitin ligase ARIH1 protects against genotoxic stress by initiating a 4EHP-mediated mRNA translation arrest

Louise von Stechow*, Dimitris Typas*, Jordi Carreras Puigvert, Laurens Oort, Ramakrishnaiah Siddappa, Alex Pines, Harry Vrieling, Bob van de Water, Leon H. Mullenders and Erik H.J. Danen

* These authors contributed equally to this work

Adapted from von Stechow et al. Molecular and Cellular Biology 2015. 2015 Apr 1;35(7):1254-68

ABSTRACT

DNA damage response signalling is crucial for the protection of the genome in all organisms and presents avenues to combat chemo- or radio-therapy resistance of cancer cells. In an RNAi screen for (de)ubiquitylases and sumoylases modulating the apoptotic response of embryonic stem (ES) cells to DNA damage, we identified the E3 ubiquitin ligase/ ISGylase, Ariadne homologue 1 (ARIH1). ARIH1 depletion sensitised ES and cancer cells to genotoxic compounds, irrespective of their p53- or caspase-3 status. Expression of wild-type, but not ubiquitylase-defective, ARIH1 constructs reversed the ARIH1-loss-induced sensitisation. ARIH1 protein abundance increased after DNA damage through attenuation of proteasomal degradation that required ATM signalling. ARIH1 associated with 4EHP and in turn, this competitive inhibitor of the translation initiation factor eIF4E, underwent increased non-degradative ubiquitylation upon DNA damage. Genotoxic stress led to an enrichment of ARIH1 in perinuclear, ribosome-containing regions and triggered 4EHP association with the mRNA 5' cap as well as mRNA translation arrest, in an ARIH1-dependent manner. Finally, restoration of DNA damage-induced translation arrest in ARIH1-depleted cells, by means of an eiF2 inhibitor, was sufficient to reinstate resistance to genotoxic stress. These findings establish ARIH1 as a potent mediator of DNA-damage-induced translation arrest that protects stem and cancer cells against genotoxic stress.

INTRODUCTION

DNA damage leads to acute toxicity, accumulation of mutations and subsequent chromosomal instability, potentially resulting in malignant transformation [1, 2]. To counteract these deleterious effects of DNA damage the cell is equipped with a highly complex signalling response termed the DNA damage response (DDR). The DDR activates effector components involved in protective pathways, including DNA damage repair, cell cycle arrest, transcription regulation, chromatin remodelling and cell death (1). The several complexes that collectively constitute the DDR are crucial for the protection of the genome in all organisms. Moreover, understanding DDR signalling in the context of chemical or ionising radiation-induced DNA damage is important to design improved strategies to combat therapy resistance. In tandem with phosphorylation-mediated signalling, which is largely executed by the PI3Kl like kinases ATM, ATR and DNA-PK, the checkpoint kinases Chk1 and Chk2, and members of the MAPK family [3, 4], protein modifications by ubiquitin and ubiquitin-like moieties are crucial at all levels of the DDR [5].

The ubiquitylation machinery can form various, differentially interpreted tags, including both degradative (K48-, K11-linked chains) and non-degradative (mono-ubiquitylation, K63-linked chains) signals [6]. In parallel, a growing family of UBiquitin-Like (UBL) proteins such as SUMO, Nedd8 and ISG15 has been identified. Covalent attachment of these UBLs on downstream targets mostly provides non-degradative signals. The ubiquitylation, sumoylation, and ISGylation systems have been shown to share several common enzymes [7-9]. Ubiquitin mediated signalling is vital to many cellular processes, including the response to DNA damage. Recognition and processing of double strand breaks (DSBs) and intrastrand crosslinks, polymerase switching during translesion synthesis (TLS), nucleotide excision repair, and p53 stability are all regulated by ubiquitylation [5, 10, 11]. More recently, ISGylation was also implicated in the DDR, as ATM-mediated deactivation of the ISG system was demonstrated to serve as a mechanism enhancing ubiquitylation-mediated

protein turnover after DNA damage [12].

Ubiquitin and ubiquitin-like modifications occur through three enzymatic steps, commencing with an E1 activating enzyme, which forms a thioester bond to the ubiquitin protein. Subsequently, the charged ubiquitin monomer is relayed to an E2 enzyme that conjugates the ubiquitin molecule to its target protein with the aid of an E3 ubiquitin ligase [13]. While there are only a few E1 and E2 enzymes, a large number of E3 ubiquitin ligases dictates substrate specificity and ensures substrate diversity of the ubiquitin system (13). There are two E3 ubiquitin ligase families. In RING ubiquitylases, the ligase functions as an adaptor between the E2 enzyme and the substrate, facilitating transfer of the ubiquitin moiety to the target protein. In HECT ubiquitylases, the ubiquitin is first conferred to a conserved residue within the HECT domain and then added to the substrate protein [14]. Recently, it was established that ubiquitin ligases of the Parkin family, including Parkin and the human homologue of Ariadne1 (ARIH1; HHARI) resemble hybrids between HECT and RING domain ubiquitin ligases [15].

In response to DNA damage, ongoing transcription and translation have to be adjusted to allow execution of stress-specific programs, save energy, accomplish DNA repair and avoid the transcription and subsequent translation of potentially mutated genetic material [16]. Genotoxic stress has been shown to induce a block in protein synthesis [17-19]. Eukaryotic mRNAs are mostly recruited to the ribosome through their 5' 7-methylguanosine cap [20]. The rate-limiting step of eukaryotic cap-dependent translation initiation is the binding of the eIF4F complex to the mRNA 5' cap structure. eIF4F is composed of the cap-binding protein eIF4E, the RNA helicase eIF4A and the scaffold protein eIF4G [21, 22]. Recruitment of additional eIF proteins and the 40S ribosomal subunit completes the pre-initiation complex that scans the mRNA for the AUG codon and drives mRNA translation initiation (20-22). If eIF4E is substituted by its structural analog 4EHP at the mRNA 5' cap, the formation of the pre-initiation complex is abolished [20]. Thus, 4EHP constitutes a negative regulator of translation initiation.

Here, we describe the identification of the Parkin family E3 ubiquitin ligase, ARIH1 in an RNAi screen for modulators of chemosensitivity. We show that

ARIH1 levels and cellular localisation are regulated in response to DNA damage. In turn, ARIH1 protects stem- and cancer cells against genotoxic compounds and γ-irradiation (IR) by promoting and fine-tuning a 4EHP-mediated mRNA translation arrest.

RESULTS

Identification of CP response modulators by an RNAi screen for ubiquitylation-family enzymes

We performed an siRNA-based screen using the Dharmacon ubiquitylation SMARTpool library and custom made SMARTpool libraries targeting all known cellular deubiquitylases (DUBs), sumoylases, and desumoylases (Table S1). Mouse embryonic stem (ES) cells that display a robust apoptotic response to genotoxic compounds including CP (Fig S1A, B), were treated with 10mM CP or vehicle and cell viability was monitored after 24h. 50 identified SMARTpools met our selection criteria [no significant effect under control conditions; modulation of viability in presence of CP with Z-score +/- 1.5 and p-value > 0.05] (Fig 1A; Table S2). As controls, we included siRNA SMARTpools targeting either Kif11, expected to already induce cell killing under control conditions due to mitotic spindle defects, or p53, expected to protect ES cells against CP-induced killing. In all experimental plates, siKif11 resulted in ~90% reduction in viability under both control and CP-treated conditions whereas sip53 protected against CP-induced loss of viability (Fig S1C). As a quality measurement, Z'-factors were calculated based on siLamin (negative control) and sip53. The average of calculated Z'-factors was 0.45, indicating a good signal to noise ratio and reproducibility of the screens (Fig S1D). To exclude off-target effects, the 50 identified SMARTpools entered a deconvolution screen, where 28/50 hits were confirmed with at least 2/4 independent sequences reproducing the effect of the SMARTpool (Fig 1B,C, Table S3).

The 28 confirmed hits included siRNAs targeting six DUBs, one E1 ubiquitin-activating enzyme, Ube1x, one E2 ubiquitin-conjugating enzyme, UBE2D3,

as well as 12 siRNAs targeting E3 ubiquitin ligases (Fig 1D). Moreover, we identified seven siRNAs targeting proteins with no described ubiquitylation-related function that were included in the ThermoFischer “ubiquitylation library” based on the presence of predicted domains associated with ubiquitylase function, such as RING, SOCS, or SPRY (see discussion). The knockdown of the E1 ubiquitin enzyme Ube1x (Uba), which has recently been shown to be a crucial E1 enzyme in the DDR following ionising radiation and replication stress [23], resulted in a particularly strong reduction of viability (Fig 1C).

Enrichment of p53-modyfiers and DNA repair regulators

A large proportion of the identified hits have been previously shown to control the levels or activity of the transcription factor p53, which acts as a master regulator of the outcome of the DDR in various cell types, including ES cells (Fig 1E) [1, 2, 24]. Three of the identified DUBs, USP7 (HAUSP), USP4, and USP5 can directly or indirectly influence p53 protein levels [10, 25-27]. In addition, the E3 ligases Rfwd3, Pirh2 and TOPORS were previously implicated in regulation of p53 stability [10, 28, 29] (Fig 1E; Table S3). Besides p53 regulators, we identified several other ubiquitin ligases involved in DDR-related processes, like post-replication repair (SHPRH [30]), translesion synthesis (Pirh2 [31]), DSB repair (BRCA1 [32]), and the RPA-mediated repair of single strand breaks (Rfwd3 [33]), further confirming the validity of the targets identified in our screen.

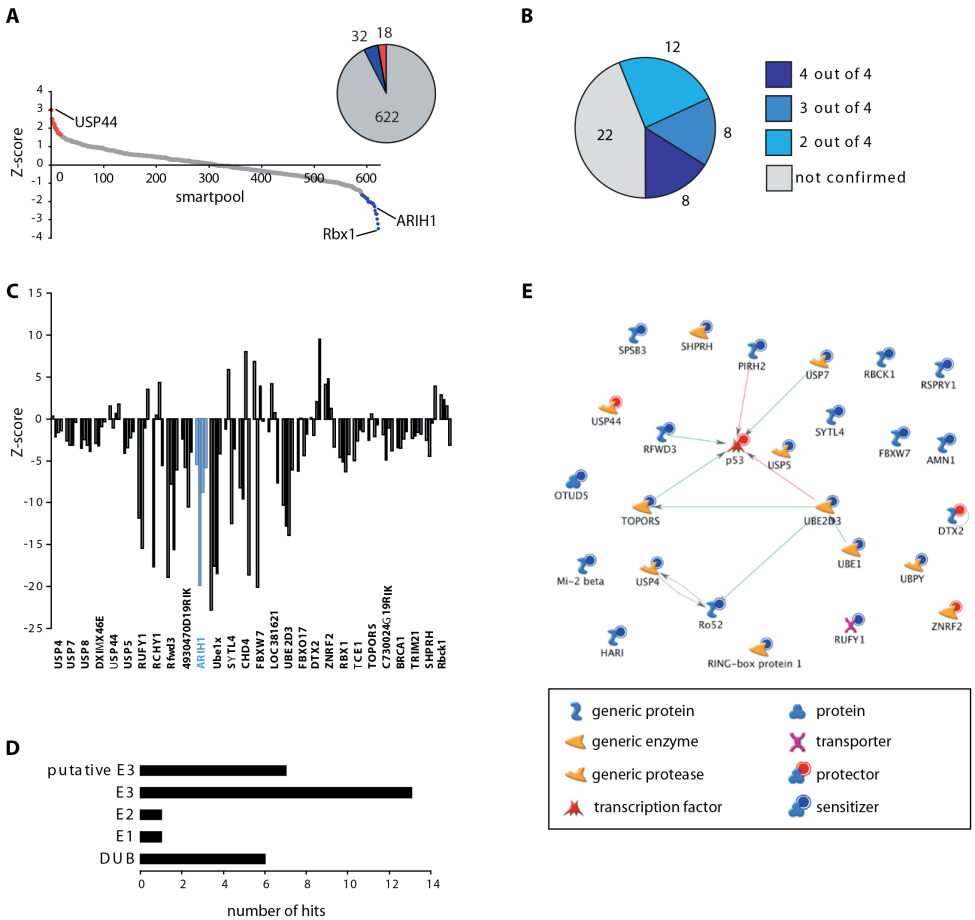

Figure 1. Identification of modulators of the CP response by an RNAi screen for ubiquitylation / sumoylation enzymes. (A) Hits identified in primary screens; protecting siRNA SMARTpools in red, sensitising siRNA SMARTpools in blue. (B) Results of deconvolution screen for 50 SMARTpools identified in primary screen. (C) Z-scores obtained for 28 confirmed hits in deconvolution screen. ARIH1 results indicated in blue. (D) Distribution of hits over different gene families as indicated. (E) Metacore-predicted network derived from screen hits; interactions with p53 are indicated. Red circles, protecting siRNAs; blue circles, sensitising siRNAs.

Silencing ARIH1 sensitises to genotoxic stress

One of the strongest obtained hits was the Parkin family ubiquitin ligase Ariadne Homologue 1 (ARIH1) [34]. The ARIH1 SMARTpool, as well as all four of the individual sequences tested in the deconvolution experiments, significantly sensitised ES cells to CP-induced loss of viability (Fig 1A,C; Table

S3). In order to examine if ARIH1 was involved in the response to specific types of stress, the effect of ARIH1 knockdown in ES cells was examined after treatment with various genotoxic and non-genotoxic compounds. All compounds were used at equitoxic doses causing ~50% loss-of-viability after 24h treatment (Fig 2A). ARIH1 depletion, using the SMARTpool or individual siRNAs, did not affect ES cell viability under control conditions (Fig 2B,C). Similar to its effect on CP-sensitivity, silencing ARIH1 using the SMARTpool or individual siRNAs significantly sensitised ES cells to all tested genotoxic drugs, including the topoisomerase inhibitor etoposide, the DNA intercalator doxorubicin, and the DNA crosslinking compound mitomycin C (Fig 2B,C). In contrast, ARIH1 loss did not sensitise ES cells to non-genotoxic agents such as the oxidative stressor diethyl maleate (DEM), the ER stressor thapsigargin (THAPS), or the microtubule poison Vincristine (VINC) (Fig 2C). Decreased viability, as measured in the ATPlite assay, correlated with an increased subG1/G0 fraction in ARIH1-depleted ES cells that could be detected after treatment with a lower dose of CP, pointing to increased cell death (Fig 2D).

In order to validate these findings in human cancer cells, we examined the effect of silencing ARIH1 in U2OS, p53 wild-type human sarcoma cells. We introduced lentiviral shRNAs targeting ARIH1 and, following bulk puromycin selection, identified two short hairpins providing ~90% reduction in ARIH1 protein levels (Fig 2E). Basal cell survival was somewhat reduced when compared to a lentiviral control cell line (Fig 2F). Nevertheless, analogous to the effect observed in ES cells, both ARIH1-depleted cell lines showed a significantly increased loss of viability in response to treatment with 10 or 25mM CP for 48h (Fig 2F). In further agreement with these findings, clonogenic survival in a colony-formation assay of ARIH1-depleted U2OS cells was also markedly more impaired by 24 hour pretreatment with a dose range of CP as compared to control cells (Fig 2G).

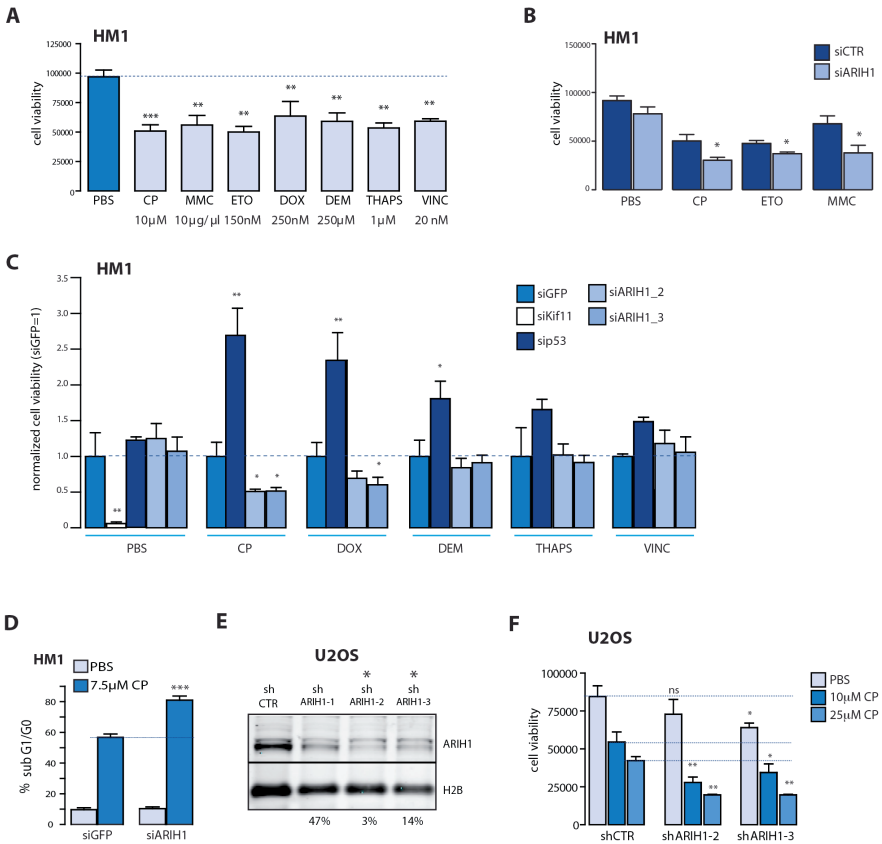

Figure 2. Silencing ARIH1 sensitises to genotoxic stress. (A) ES cell viability after treatment for 24 hours with indicated equitoxic concentrations of CP, mitomycin C (MMC), etoposide (ETO), doxorubicin (DOX), diethylmaleathe (DEM), thapsigargin (THAPS), or Vincristine (VINC). (B) ES cell viability in presence of control or ARIH1 siRNA after treatment with equitoxic concentrations of CP, ETO, or MMC. (C) ES cell viability in presence of Kif11-siRNA (only for PBS), GFP-siRNA, p53-siRNA, or 2 individual siRNA sequences targeting ARIH1 after treatment with equitoxic concentrations of CP, DOX, DEM, THAPS or VINC (normalised to siGFP). (D) Sub-G1/G0 apoptotic fraction of control or siARIH1 ES cells treated with 7.5mM CP for 24h. (E) ARIH1 protein levels and H2B loading control in U2OS cells bulk puromycin-selected for expression of shcontrol or 3 individual shRNAs targeting ARIH1. Percentages indicate remaining ARIH1 expression. Asterisks indicate shARIH1 #2 and #3 used in all further experiments. (F) U2OS cell viability in shcontrol or 2 individual shARIH1 cell lines after treatment with vehicle (PBS) or 10 or 25mM CP for 48h. (G) Colony formation capacity in shcontrol or shARIH1-2 and -3 U2OS cell lines after 24h treatment with CP at indicated concentrations. *p<0.05; **p<0.01, ***p<0.001 (students t-test).

Genotoxic stress-induced ARIH1 accumulation represents a p53- and caspase-3-independent adaptive response

In contrast to reported functions for many of the other identified hits (Fig 1E, Table S3), ARIH1 did not control basal or genotoxic stress-induced p53 stability in ES or U2OS cells (Fig 3A,B). In further disagreement with a role for p53 in the enhanced sensitivity to genotoxic stress observed in ARIH1-depleted cells, silencing ARIH1 effectively sensitised the p53-deficient non-small-cell lung cancer cell line H1299 [35] to CP (Fig 3C,D). Transient knockdown of ARIH1 also sensitised the caspase-3 deficient human breast cancer cell line MCF7, indicating that the effect of ARIH1 was not restricted to caspase 3-mediated apoptosis (Fig 3E). Although less prominent, the same effect was observed using 2 independent MCF7 shARIH1 lines (Fig 3F,G). DNA damage can trigger a p53-dependent or independent cell cycle arrest [36]. In MCF7, ARIH1 loss did not alter the basal cell-cycle distribution or the CP-induced increase of S/G2 populations (Fig 3H,I). Likewise, ARIH1 knockdown did not affect the basal cell-cycle distribution or the CP-induced G2/S arrest in ES cells (Fig 3J,K). Together, these data indicate that ARIH1-depleted cells display normal cell-cycle arrest in response to genotoxic stress, while cell survival upon DNA damage is compromised in the absence of ARIH1, with this increased sensitivity being independent of p53 or caspase-3-mediated apoptosis.

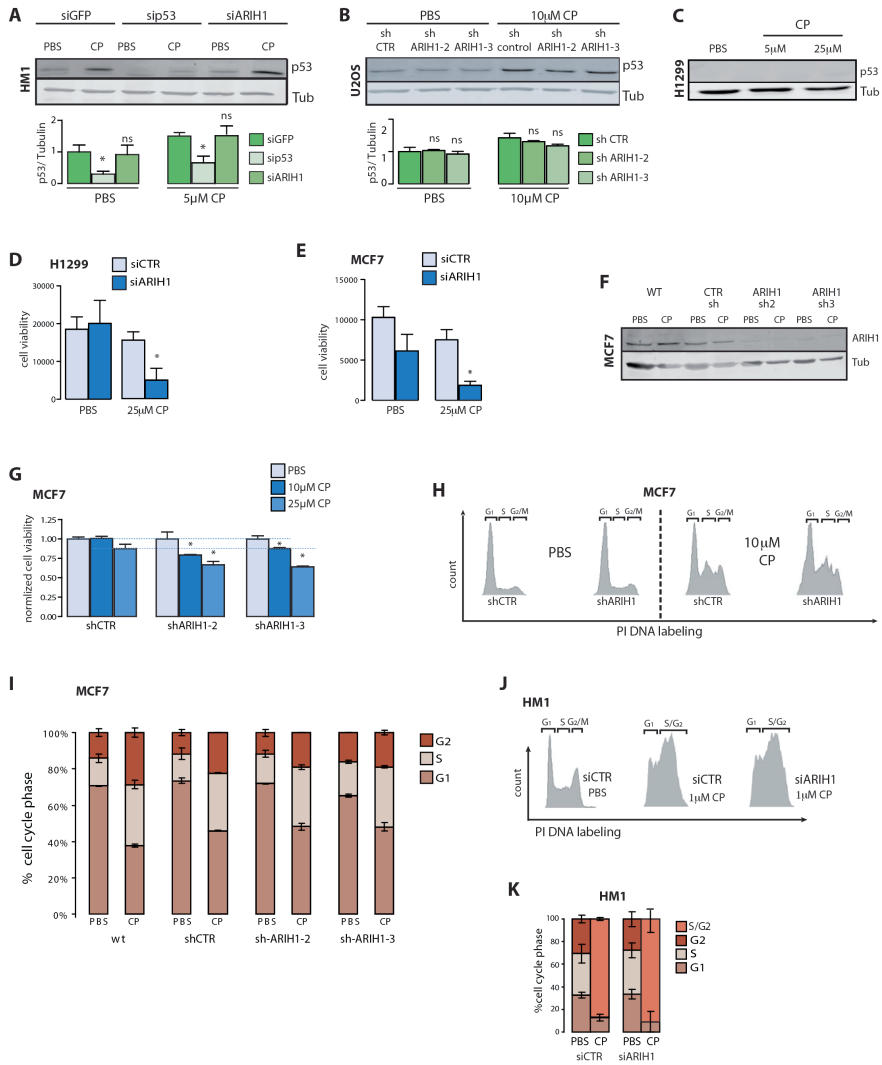

Figure 3. Silencing ARIH1 enhances cell death in response to genotoxic stress in a p53 and caspase-3 independent manner. (A) p53 and tubulin control protein levels in ES cells in presence of indicated siRNAs treated with PBS control or 5mM CP for 8h (n=4). (B) p53 and tubulin control protein levels in U2OS cells in the presence of the indicated shRNAs treated with PBS control or 10mM CP for 16h (n=3). (C) p53 and tubulin control protein levels in p53-deficient H1299 cells treated with indicated concentrations of CP for 24h. Note absence of p53. (D) H1299 cell viability under control or siARIH1 conditions after treatment with vehicle control PBS or 25mM CP for 24h. (E) MCF7 cell viability under control or siARIH1 conditions after treatment with PBS or 25mM CP for 48h. (F) ARIH1 and tubulin control protein levels in MCF7 cells in the presence of the indicated shRNAs (G) Cell viability for shcontrol and two shARIH1 MCF7 cell lines treated for 48h with PBS, 10 or 25mM CP. (H) FACS analysis for cell cycle content in shcontrol and shARIH1 MCF7 cell lines treated for 24h with PBS or 10μM CP. (I) Quantification of cell cycle profiles in wt, shcontrol and shARIH1-2 and -3 MCF7 cell lines after treatment with PBS or 10mM CP for 24h. (J) FACS profiles for HM1 cell cycle content under control, siGFP, or siARIH1 conditions after treatment with vehicle control or 1μM CP. (K) Cell cycle distribution derived from profiles in J (n=3). *p<0.05.

Subsequently, we tested if DNA damage affected the abundance of ARIH1. ARIH1 protein levels were boosted following CP treatment in U2OS cells (Fig 4A). This could not be explained by elevated mRNA levels, indicating that genotoxic stress triggered either increased synthesis or enhanced stability of the ARIH1 protein (Fig 4B). Treatment with the proteasome inhibitor MG132 led to increased basal ARIH1 levels, with CP treatment not causing further ARIH1 accumulation under these conditions (Fig 4C). KU-5593, an inhibitor of ATM, a central kinase within the DDR signalling network, blocked CP-induced ARIH1 accumulation, suggesting that DNA-damage caused ATM-mediated attenuation of proteasomal degradation of ARIH1 (Fig 4C). We then sought to address whether regulation of ARIH1 abundance might occur through suppression of self-ubiquitylation. Although ARIH1 indeed appeared to be ubiquitylated, this modification was not regulated by CP and was unaffected by ATM inhibition (Fig S2A). Moreover, a ubiquitylation-deficient ARIH1 mutant (C208A) displayed a markedly similar ubiquitylation pattern (Fig S2A) (24). Notably, by MS analysis of GFP-ARIH1 immuno-precipitations we identified K144 as a ubiquitylated site in ARIH1, yet this was not modulated by CP treatment (Fig S2B). We also identified multiple ARIH1-interacting components of the ubiquitylation machinery (i.e. ubiquitin itself, the E1 enzyme UBA1, and the E2 enzyme UBE2L3 known to interact with ARIH1). Such interactions, as well as a potential product (K48 poly-ubiquitin chains), were moderately increased upon CP treatment (Fig S2B).

CP treatment induces 4EHP ubiquitylation

In response to DNA damage, ongoing cellular activities are suppressed while stress programs and DNA repair processes are activated. One aspect of the DNA damage response is the acute inhibition of protein synthesis through alterations of the cap-dependent translation initiation complex [37]. This can be achieved in several ways, including cap-recruitment of 4EHP (eIF4E2), a competitive inhibitor of the canonical cap-binding translation initiation factor, eIF4E [20]. In contrast to eIF4E, 4EHP cannot bind the structural component eIF4G that is required for ribosome accrual and subsequent mRNA translation. Although ARIH1 can act as an E3 ubiquitin ligase for 4EHP [38], there is also evidence that ARIH1 can ISGylate 4EHP, thus enhancing its

affinity for the mRNA cap structure and its ability to replace eIF4E [39]. Co-immunoprecipitations in U2OS cells showed that the increased abundance of ARIH1 in CP-treated cells was accompanied by increased association of ARIH1 with 4EHP and this 4EHP-associated ARIH1 was lost in shARIH1 cells (Fig 4D,E).

Furthemore, we analysed CP-induced posttranslational modification of wild-type 4EHP and a [K121/130/134/222R]-mutant (4KR) that cannot be ISGylated [39]. Immunoprecipitation of wild -ype 4EHP showed bands of higher molecular weight appearing upon CP treatment (Fig 4F). Identical bands were also observed for the 4KR-4EHP mutant arguing against a CP-induced 4EHP-ISGylation. Moreover, such species were detected by a ubiquitin antibody, whereas Western blotting for co-expressed HA-ISG15 did not detect these species, despite the fact that free ISG15 was readily detected in the FLAG immunoprecipitations. The most prominent modification corresponded to mono-ubiquitylated 4EHP (28+7 kDa) although the ubiquitin Western blot indicated that 4EHP di-ubiquitylation may also occur.

ARIH1 ubiquitylation function mediates adaptation to genotoxic stress

Results thus far suggested that 4EHP is ubiquitylated, not ISGylated, after genotoxic stress. We tested whether the ISGylation or ubiquitylation function of ARIH1 was required for its protective role in genotoxic stress. Therefore, we silenced endogenous ARIH1 using an siRNA targeting the 3' UTR in U2OS cells expressing either exogenous wild-type ARIH1 or a C208A mutant that fails to associate with the E2 enzyme UbcH7, rendering it defective in ubiquitylation (whereas interaction with UbcH8 and hence, ISGylase activity remains intact) [40]. In agreement with earlier findings, ARIH1-silenced cells were more sensitive to CP treatment although the effect of the transient siRNA was less prominent than stable shRNA-mediated silencing (see Fig 2G). More importantly, expression of wild-type- but not ubiquitylation-deficient (C208A) ARIH1, restored colony formation capacity under genotoxic stress in cells depleted for endogenous ARIH1 (Fig 4G). Put together, these data indicate that 4EHP ubiquitylation constitutes the predominant modification induced by genotoxic stress, with the ubiquitylase function of ARIH1 being crucial for its protective role in the genotoxic stress response.

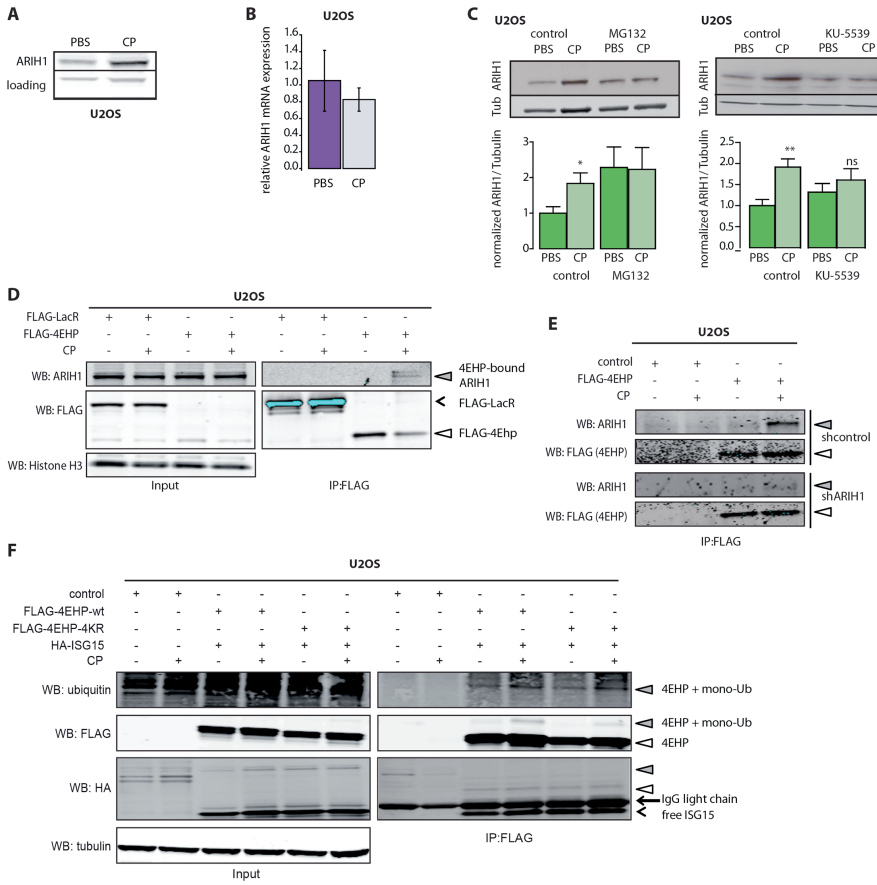

Figure 4. ARIH1 accumulates after DNA damage and interacts with 4EHP. (A) ARIH1 protein levels in U2OS cells treated for 4h with PBS or 5mM CP. (B) qPCR analysis of ARIH1 RNA levels, normalised to GAPDH in U2OS cells treated for 4h with PBS or 5mM CP. (C) Western blot for ARIH1 and tubulin loading control. For inhibitor treatment, cells were pretreated for 30min with DMSO vehicle control, 10mM proteasome inhibitor MG132, or 5mM ATM inhibitor KU-55933 and subsequently exposed to 5mM CP or PBS vehicle control for 4h in the presence of indicated inhibitors (n=4). (D) Total cell lysates and FLAG pull-down of U2OS cells transfected with control FLAG-LacR or FLAG-4EHP with vehicle control or 5μM CP for 4h. Blots were probed for FLAG, ARIH1 and Histone H3 (loading control). (E) FLAG pull-down of U2OS cells in the presence of the indicated shRNAs, subsequently transfected with control (empty) or FLAG-4EHP cDNAs, and treated with vehicle control or 5μM CP for 4h. Blots were probed for 4EHP (FLAG) and ARIH1. Open and shaded arrowheads as explained in D. (F) Total cell lysates and FLAG pull-down of U2OS cells transfected with FLAG-4EHP (wt or 4KR) in combination with HA-ISG15 and treated with vehicle control or 5μM CP for 4h. Blots were probed for FLAG, HA, ubiquitin and tubulin (loading control) (G) Colony formation capacity after 24h treatment with CP at indicated concentrations in control U2OS cells or U2OS cells stably expressing GFP-tagged wild-type or C208A mutant ARIH1, in absence or presence of siRNA targeting luciferase (control) or the ARIH1 3'UTR. * p<0.05.

CP-treatment induces 4EHP cap-binding and translation arrest in an ARIH1-dependent manner

ARIH1-dependent ISGylation has been reported to regulate 4EHP association with the mRNA 5' cap but ARIH1-mediated ubiquitylation of 4EHP, although described, is not known to affect this process. In order to clarify whether ARIH1 supported 4EHP translocation to the mRNA cap upon CP treatment, we utilised 5' 7-methylguanosine cap-pulldown assays. Indeed, 4EHP binding to the mRNA cap was induced in response to CP in U2OS, MCF7, as well as ES cells (Fig 5A-D). Importantly, this response was dependent on ARIH1 as the CP-induced 4EHP:cap association was abrogated in U2OS, MCF7, and ES cells upon ARIH1 depletion (Fig 5A-D). Subsequently, to test if the 4EHP:cap association represents an ARIH1-regulated pathway that is involved in protection against CP, 4EHP itself was silenced. In line with such a protective function, ES cells and U2OS cells were sensitised to genotoxic compounds following 4EHP silencing, while viability of H1299 in presence of CP and control conditions was compromised (Fig 5E-H).

These findings hint that the ability of ARIH1 to protect against genotoxic stress-induced cell death involves 4EHP-mediated translation inhibition at the mRNA 5' cap. To address whether ARIH1 localised at sites of mRNA translation upon genotoxic stress, we performed immunostainings to assess subcellular distribution of ARIH1. Whereas in untreated U2OS cells ARIH1 resided in the nucleus and diffusely throughout the cytoplasm, treatment with CP or IR caused ARIH1 accumulation at both the nucleus and speckled structures in perinuclear regions, which markedly resemble ribosomes (Fig 5H). In agreement with a genotoxic stress-induced transittion of ARIH1 to ribosomes, and a role in 4EHP-mediated translation arrest, eIF4G2, a ribosomal marker, co-localised to such ARIH1-containing perinuclear regions upon either CP treament or IR (Fig 5I,J).

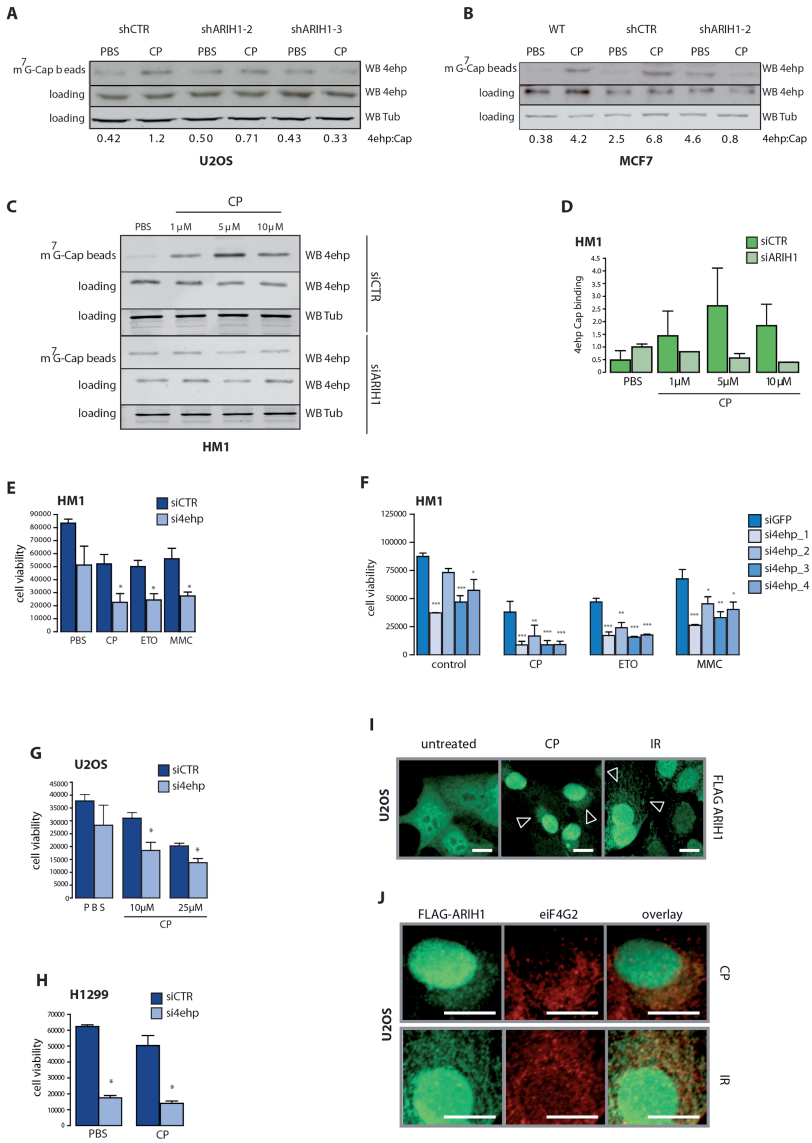

Figure 5. ARIH1 mediates DNA damage-induced cap binding of 4EHP. (A-C) m7G-cap pulldown from control and ARIH1-silenced U2OS (A), MCF7 (B) or HM1 ES cells (C) treated with vehicle control or indicated concentrations of CP. Blots were probed for 4EHP and tubulin (loading control). Numbers at the bottom of A and B indicate cap-associated 4EHP levels relative to total 4EHP. (D) Quantification of m7G-cap-bound 4EHP in ES cells treated with indicated siRNAs (n=2). (E) ES cell viability in the presence of the indicated siRNAs after treatment with PBS, 10mM CP, 150nm ETO, 10mg/ml MMC for 24h. (F) ES cell viability in the presence of the indicated siRNAs after treatment with vector, 10mM CP, 150nm ETO or 10mg/mL MMC. (G) As in (F) but for U2OS after treatment with PBS, 10 or 25μM CP. (H) As in (F) for H1299 cells after treatment with PBS or 25μM CP. (I) FLAG-ARIH1 localisation before or after treatment with 5μM CP for 4h or 4h after treatment with 2Gy IR. Arrowheads indicate regions of perinuclear accumulation. (J) Higher magnification of perinuclear staining for FLAG-ARIH1 (green), ribosomal marker eiF4G2 (red) staining after CP treatment or IR. *p<0.05; **p<0.01.

To directly address whether ARIH1 was important for inducing a DNA damage-induced translation arrest, Click-iT® metabolic labelling was used to quantify newly synthesised proteins. CP treatment caused a significant translation arrest in U2OS cells with a 30% reduction of protein synthesis at 2h post-treatment and maintenance of a 25% reduction at 4 and 8h post-treatment (Fig 6A). In line with a critical role for ARIH1 in mediating this arrest, two independent shARIH1 lines did not show this CP-induced translation arrest. Notably, a 60% reduction in translation caused by cyclohexamide in wild-type U2OS remained intact in ARIH1-silenced cells (Fig 6A,B).

Finally, we investigated if the ARIH1-mediated translation arrest was critical for the role of ARIH1 in adaptation to genotoxic stress. For this, we made use of salubrinal, an inhibitor of eIF2a dephosphorylation that renders the eIF2 initiation factor inactive and inhibits mRNA translation under stressed conditions. Co-treatment with salubrinal restored the CP-induced translation arrest in ARIH1-depleted cells (Fig 6B). Indeed, such an alternatively triggered translation arrest significantly restored viability of CP-treated ARIH1-silenced U2OS, ES and MCF7 cells (Fig 6C-E).

Altogether, these findings support a model in which DNA damage induces an increase in ARIH1 protein levels and an association of ARIH1 with 4EHP. In turn, this causes 4EHP recruitment to the mRNA cap where it is known to compete with eIF4E. The resulting mRNA translation arrest represents an adaptive response to genotoxic stress: ARIH1 depletion sensitises cells to genotoxic stress while reestablishing the translation arrest at the level of eIF2 with salubrinal alleviates this effect (Fig 6F).

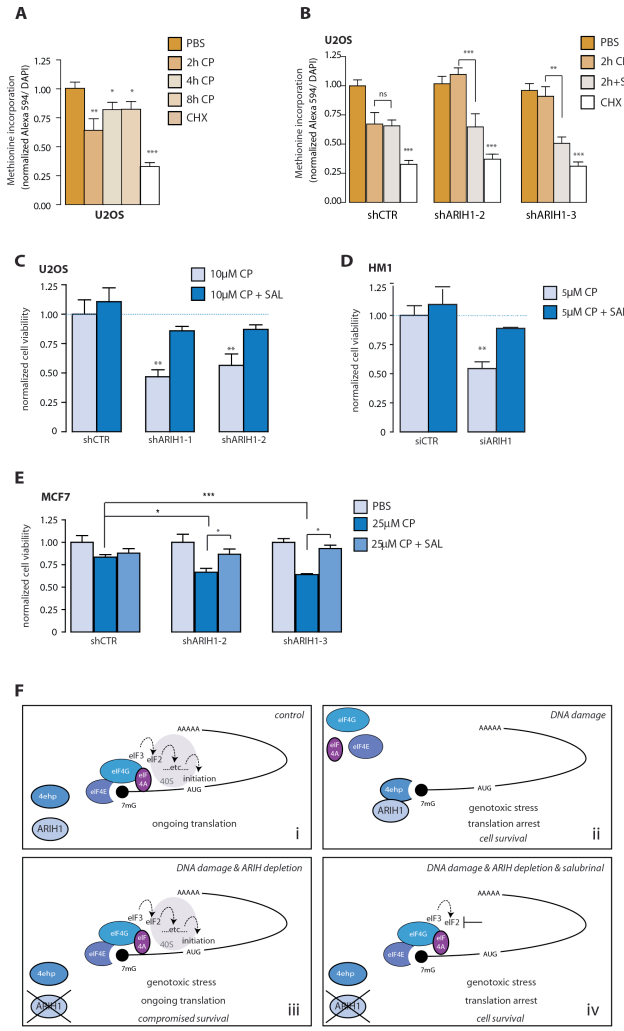

Figure 6. ARIH1 mediates CP-induced mRNA translation arrest. (A) Methionine incorporation in U2OS cells after treatment with 15mM CP for 2h, 4h or 8h or 2mg/ml cyclohexamide (CHX) for 1h. Alexa546 signal (reflecting newly synthesised protein) / number of nuclei (DAPI), normalised to PBS condition is shown. (B) As in (A) but in the presence of the indicated shRNAs and after treatment with 2mg/ml CHX for 1h, 15μM CP for 2h, or co-treatment with 15μM CP and 2.5mM salubrinal (SAL) for 2h. Alexa546 signal / number of nuclei, normalised to PBS condition is shown. (C-E) Cell survival in cells treated with the indicated siRNAs or shRNAs after treatment with indicated concentrations of CP (hr treatment) in absence or presence of 2.5mM SAL. C, U2OS 48; D, ES cells 24h; E, MCF7 48h. (F) Model for the role of ARIH1 in regulating sensitivity to genotoxic stress. i) Under non-stressed conditions, eIF4E binds the mRNA m7G-cap, a pre-initiation complex is formed scanning the mRNA until the AUG codon is found. ii) Upon genotoxic stress, ARIH1 associates with 4EHP, resulting in recruitment of 4EHP to the 5' cap where it replaces eIF4E, resulting in a cytoprotective translation arrest. iii) In the absence of ARIH1, 4EHP is not recruited to the mRNA 5' cap, DNA damage-induced translation arrest does not occur, and cell survival is compromised. iv) Restoration of translation arrest in ARIH1-depleted cells by preventing formation of a pre-initiation complex through inhibition of eIF2 also restores cell survival.

DISCUSSION

Ubiquitylation plays a vital role in the DDR signal transduction cascade. Our RNAi screen targeting the cellular ubiquitylation and sumoylation machinery helped us identify several genes that modulate the response to the chemotherapeutic drug CP. Some of the identified DUBs and E3 ubiquitin ligases have been previously implicated in p53 regulation or DNA repair processes [5, 10]. In addition, through our screen we picked up genes associated with cell cycle control or developmental processes. These include Fbxw7, a tumour suppressor that marks several proto-oncogenes, such as Myc, Jun, cyclin E, and Notch for degradation; and Dtx2, an E3 ligase also proposed to control the Notch signalling pathway [41-43]. Which of these functions explains the role of these ubiquitin ligases in the response to genotoxic stress is not known. Moreover, while two of the individual siRNAs mimicked the SMARTpool for these genes, the deconvolution screen also revealed one individual siRNA for these genes to have the opposite effect. This indicates that either of those outcomes is likely an off-target effect and further experiments are required to determine the role of these genes in the response to genotoxic stress. We also identified another F-box protein, Fbx017, where the SMARTpool and 3/4 individual siRNAs caused sensitisation, thus bestowing more confidence in a potential role of this gene in adaptation to genotoxic stress. However, no mechanism of action has been described for Fbx017 yet.

Another group of identified hits has been associated with intracellular transport processes, including the DUB USP8, which regulates endosomal sorting of membrane receptors and RUFY and SYTL4, which are involved in Rab-mediated vesicular transport [44-46].Notably, some of the hits from the “ubiquitylation SMARTpool library” do not have established (de)ubiquitylase function. These include i) the Zinc finger-containing chromatin remodeling factor CHD4 that lacks domains associated with (de)ubiquitylase activity [47]; ii) the Rab-interacting proteins RUFY and SYTL4 that have a FYVE-Zinc finger domain, which is structurally similar to the RING domain [45,

46]; and iii) TCE1 and Rspry1, containing a SPRY domain that is found in members of the TRIM-family of ubiquitin ligases [48]. In addition, Rspry1 contains a RING domain and TCE1 also harbors a SOCS box domain, which mediates interactions with the Elongin BC complex, an adapter module in E3 ubiquitin ligase complexes [49].

The Parkin family ubiquitin ligase, ARIH1 has not been previously implicated in DDR signalling. Our findings reveal that ARIH1 protects pluripotent stem cells, as well as various cancer cells, from the toxic effects of genotoxic chemical agents that cause DSBs. The cytoprotective role of ARIH1 is also observed in cancer cells lacking a functional p53 or caspase-3 response. Hence, ARIH1 is not required specifically for dampening p53-induced, caspase-3-mediated apoptosis. Instead, we find that ARIH1 mediates an mRNA translation arrest in response to DNA damage by binding to 4EHP and stimulating its recruitment to the mRNA 5' cap.

The temporary arrest of mRNA translation is an important event in the response to cellular stress and alterations in this regulatory hub have been suggested to be important for resistance of cancer cells to therapy [19, 50]. A well-described mechanism for translation repression is the enhanced interaction of the cap-binding protein eIF4E with its negative regulator eIF4-BP1. Under normal conditions this interaction is suppressed by mTOR-mediated phosphorylation of eIF4-BP1 [51]. Alternative eIF4E-dependent and independent mechanisms for translation repression have also been described [20]. For instance, impaired Met t-RNA recruitment, through eif2a Ser51 phosphorylation, represents a canonical response to accumulation of improperly folded proteins in the endoplasmic reticulum; the so-called unfolded protein response [52]. Yet another way to arrest mRNA translation is through enhanced mRNA 5' cap-binding of eIF4E2, also known as 4EHP [53]. Our findings implicate this latter mechanism in the DNA damage-induced protein synthesis arrest and provide evidence that it is regulated through ARIH1.

4EHP is an eIF4E homologue that has low affinity for binding the cap structures of most mRNAs [54]. The protein has been implicated in the regulation of translation of a specific subset of mRNAs in Drosophila involved in embryonic

patterning [55, 56]. ARIH1 can ISGylate 4EHP, thus leading to increased mRNA 5' cap affinity, but it is not known under which conditions ARIH1-mediated ISGylation of 4EHP is induced [39]. Here, we demonstrate that in response to DSB-inducing genotoxic stress, ARIH1 protein accumulates and interacts with 4EHP, leading to increased recruitment of 4EHP to the mRNA 5' cap. Our findings using a non-ISGylatable 4EHP mutant and 4EHP:ISG15 co-immunoprecipitations, indicate that ubiquitylation, not ISGylation is the predominant DNA damage-induced 4EHP modification. Moreover, we show that ubiquitylation capacity is required for the ARIH1-mediated adaptive response to genotoxic stress.

The accumulation of ARIH1 depends on activity of ATM, a key kinase in the DDR, and most likely involves inhibition of proteasomal degradation. Despite a putative ATM target motif (S-Q) in the ARIH1 protein at Serine 514, phosphorylation of this site has not been detected by us or by other groups in the presence or absence of genotoxic stress (unpublished data; [3, 57, 58]; http://www.phosphosite.org). Although this may be an outcome of technical limitations of MS used in these studies (for example a very short tryptic fragment), it points to an indirect mechanism by which ATM signalling leads to increased ARIH1 expression after genotoxic stress. One possible mechanism would involve attenuation of ARIH1 self-ubiquitylation following genotoxic stress. However, our results do not suggest auto-ubiquitylation, or its regulation by genotoxic stress or ATM, as the relevant mechanism. It is worth mentioning that our MS analysis indicates that ARIH1 is primarily part of a complex of ubiquitylation-related enzymes. The detailed composition of this complex and its regulation in response to genotoxic stress will be the topic of further study.

Translation arrest is effectuated by 4EHP due to its capacity to act as a competitive inhibitor for eIF4E. Unlike eIF4E, 4EHP cannot interact with the scaffolding protein eIF4G, which is required for formation of the pre-initiation complex. In line with this, 4EHP cannot complement eIF4E in gene knockout experiments in yeast [59]. Our following findings indicate that ARIH1-mediated recruitment of 4EHP to the mRNA 5' cap underlies the cytoprotective role of ARIH1: i) DNA damage-induced recruitment of

4EHP to the mRNA 5' cap is ARIH1-dependent, ii) DNA damage-induced translation arrest is ARIH1-dependent, and iii) RNAi targeting ARIH1 or 4EHP sensitises ES or cancer cells to DNA damage. In H1299 cells, 4EHP depletion also compromises viability under control conditions, which may be related to endogenous genotoxic stress. Our data do not support the notion that a genotoxic stress-induced mRNA translation arrest is lost in cancer cells, as was described for other eIF4E dependent routes, such as 4EBP-1 phosphorylation [19]. U2OS cells do attenuate protein synthesis following genotoxic stress and depletion of ARIH1 leads to sensitisation of all cancer cell lines tested thus far. Intriguingly, while inhibition of eIF4E cap binding can sensitise cancer cells to different chemotherapeutics [19, 50], we show that inhibition of the competitive process involving ARIH1 and 4EHP has the same effect. Clearly, ongoing mRNA 5' cap-mediated translation, as well as the ability to temporarily halt translation in response to DNA damage is required for (cancer) cells to escape genotoxic stress-induced death. Our immunofluorescence experiments indicate that upon genotoxic stress, ARIH1 is increasingly concentrated in nuclei and perinuclear regions where ribosomes cluster, placing ARIH1 at the correct location to control this process.

As mentioned above, an alternative route to attenuate protein synthesis is through eiF2a Ser51 phosphorylation, a modification typically triggered by accumulation of misfolded proteins in the ER [52]. This response can be enhanced by salubrinal, an inhibitor of the phosphatase complex that dephosphorylates eIF2a [60]. Interestingly, treatment with salubrinal restores the CP-induced translation arrest and the subsequent cellular survival in ARIH1-depleted cells. This shows that alternative means for restricting protein synthesis can compensate for the inability to do so through enhanced 4EHP:cap binding. Moreover, it provides further evidence in favour of a model showing that the ability of ARIH1 to couple DSB-induced genotoxic stress to attenuation of mRNA translation underlies its cytoprotective role.

MATERIAL AND METHODS

Cell culture, plasmids and other reagents

HM1 mouse ES cells derived from OLA/129 genetic background (provided by Dr. Klaus Willecke, University of Bonn GE) were maintained under feeder free conditions in GMEM medium containing $5x10^5$U mouse recombinant leukemia inhibitory factor (LIF; PAA). All other cell lines were purchased from ATCC. MCF7 human breast cancer cells and H1299 human non-small cell lung cancer cells were maintained in RPMI medium. U2OS human sarcoma cells were kept in DMEM. All media contained 10% FBS and 25U/ml penicillin, and 25µg/ml streptomycin. All cell lines, including stable shRNA expressing derivatives, were confirmed to be mycoplasma-free using the Mycosensor kit from Stratagene.

Wild-type (#17342) and non-ISGylatable [K121/130/134/222R]-mutant (4KR) (#17353) FLAG-tagged versions of 4EHP, as well as HA-tagged ISG15 (#12444) were provided by Dr. Dong-Er Zhang, Scripps Research Institute, La Jolla CA - through Addgene [39]. By means of site-directed mutagenesis, a point mutation (C208A) was introduced into wild-type ARIH1 cDNA, yielding an ubiquitylation-deficient ARIH1 mutant [40]. Wild-type and C208A ARIH1 cDNAs were cloned into entry vector pENTR4-GFP-C1 (#w392-1) provided by Dr. E. Campeau, University of Massachusetts Medical School, Worcester, MA - through Addgene [61]. Subsequently, they were recombined into pLenti6.3 V5-DEST (Invitrogen) using Gateway® recombination. Destination vectors containing such GFP-tagged ARIH1 versions were used for either direct overexpression in mammalian cells or lentiviral production.

Genotoxicants included the DNA cross-linkers cisplatin (CP; Cis-$PtCl_2(NH_3)_2$) (provided by the Pharmacy unit of University Hospital, Leiden NL) and mitomycin C (Sigma), as well as the inhibitors of topoisomerase II-mediated DNA unwinding, doxorubicin (Sigma) and etoposide (Sigma). Oxidative stressor diethyl maleate (DEM), microtubule-poison Vincristine, and ER-stressor Thapsigargin were also obtained from Sigma. The pan-caspase inhibitor z-Val-Ala-DL-Asp-fluoromethylketone (z-VAD-fmk) was purchased from Bachem, the eif2a dephosphorylation inhibitor salubrinal was from

Calbiochem. ATM inhibitor KU-5593 and proteasome inhibitor MG132 were acquired from Tocris Biosciences. Antibodies against p53 and phospho-p53(Ser15) were purchased from Novacostra and Cell signalling, respectively. Antibodies against tubulin and FLAG were obtained from Sigma. Antibodies against mouse or human 4EHP and eIF4G2 were from Cell Signalling. ARIH1 antibody was from Novus Biologicals. Monoclonal antibody against ubiquitin was purchased from Enzo-Biosciences (FK2 clone).

RNAi experiments

siRNAs were purchased from ThermoFisher Scientific. For primary screens, the Dharmacon siGENOME SMARTpool siRNA Library- Mouse Ubiquitin Conjugation Subsets 1 (G-015610), 2 (G-015620) and 3 (G-015630) were used. For Deubiquitylation and SUMOylation-screens customised siGENOME SMARTpool siRNA libraries were used (Table S1). For deconvolution confirmation screens, customised libraries containing 4 individual siRNAs targeting each selected mRNA were used. GFP, Lamin A/C, and RISC free control siRNAs were used according to MIARE guidelines. Kif11 siRNA was used as transfection efficiency control.

The siRNA screens were performed on a Biomek FX (Beckman Coulter) liquid handling system. 50nM siRNA was transfected in 96 well plates using Dharmafect1 transfection reagent (ThermoFisher Scientific). The medium was refreshed every 24h and cells were exposed to indicated compounds or vehicle controls 64h post-transfection for 24h. Primary screens were done in duplicate and deconvolution screens were done in quadruplicate. As readout, a cell viability assay using ATPlite 1Step kit (Perkin Elmer) was performed according to the manufacturer's instructions followed by luminescence measurement using a plate reader.

For stable gene silencing, cells were transduced using lentiviral TRC shRNA vectors at MOI 1 (LentiExpressTM; Sigma-Aldrich; Dr. Rob Hoeben and Mr Martijn Rabelink, University Hospital, Leiden NL) according to the manufacturer's procedures and bulk selected in medium containing 2.5µg/ml puromycin. Control vector expressed shRNA targeting TurboGFP. shRNAs targeting ARIH1 were CCAGATGAATACAAGGTCATC

(shARIH1#1), CTACCTTGAACGAGATATTTC (shARIH1#2), CTGTTAAATGTAAGTGGTTAC (shARIH1#3). For ARIH1 gene silencing in combination with ectopic expression of GFP-ARIH1 constructs, an siRNA targeting the 3'UTR (GCACACAGCUGUAGGCAUUUU) of ARIH1 was used (ThermoFisher Scientific).

RNAi screen data analysis

As a quality control Z'-factors were determined for each plate, using Lamin A/C as a negative control and p53 as a positive control. To rank the results, Z-scores were calculated using as a reference i) the mean of all test samples in the primary screen and ii) the mean of the negative control samples in the secondary deconvolution screen (in order to prevent bias due to pre-enrichment of hits) [62]. Hit determination was done using Z-scores with a cut off value of 1.5 below or above the reference and p-value lower than 0.05. Enrichment of canonical pathways and formation of p53/ ubiquitylation signalling network was performed using MetaCore™ data-mining software.

Apoptosis and cell cycle analysis

ES cells were exposed to vehicle or CP for 8h for cell cycle analysis or 24h for apoptosis analysis. MCF7 cells were exposed for 24h for cell cycle analysis. Floating and attached cells were pooled and fixed in 80% ethanol overnight. Cells were stained using PBS EDTA containing 7.5mM propidium iodine and 40mg/ml RNAseA and measured by flow cytometry (FACSCanto II; Becton Dickinson). The amount of cells in the different cell cycle fractions or in sub G0/G1 for apoptotic cells was calculated using BD FACSDiva software. Alternatively, apoptosis was determined using live imaging of Annexin V labelling, as described previously [63].

Clonogenic survival assay

U2OS cells (250 cells/plate) expressing different shRNAs were seeded in triplicate in 9cm plates. The following day, cells were treated for 24h with a dose range of CP or IR. After a recovery period of 10 days, surviving cells were fixed, stained and colonies were counted to assay each cell-line's clonogenic potential.

Western blot analysis

Extracts were prepared in Tris/Sucrose/EDTA buffer containing protein inhibitor cocktail and separated by SDS-PAGE on polyacrylamide gels, transferred to PVDF membranes, and membranes were blocked using 5% BSA. Following incubation with primary and secondary antibodies signal was detected using a Typhoon™ 9400 from GE Healthcare.

Immunofluorescence

U2OS cells were seeded on glass coverslips and allowed to grow for two days. Subsequently, they were treated with CP and fixed using 2% formaldehyde for 20min at the indicated time-points. After washing extensively and rehydrating in PBS, post-fixation extraction took place by incubating with 0.25% Triton-X for 5min. Cells were extensively washed with PBS to remove any detergent and then blocked in 5% BSA. Finally, coverslips were immunostained with mouse anti FLAG and rabbit anti eiF4G2 antibodies and appropriate secondary fluorescent antibodies.

Cap binding assay

HM1 ES cells, U2OS, and MCF7 breast cancer cells were seeded in 6-well plates at a density of 0.5 million cells/ well. Cells were treated with different concentrations of CP for 4h (U2OS, MCF7) or 8h (ES) and proteins were harvested in lysis buffer containing 1mM phenylmethylsulfonyl fluoride (Cell Signalling). Cap binding proteins were precipitated using 7-methyl-GTP-Sepharose 4B beads (Amersham) as described previously [64]. Precipitated proteins were separated on 12% SDS-PAGE gels and analysed by immunoblotting for 4EHP (EIF4E2).

Metabolic labelling for detection of translational changes after CP treatment

Click-iT® metabolic labelling reagents for proteins was purchased from Invitrogen and used according to manufacturer's instructions. In short, U2OS cells were seeded to 80% confluence in 96 well mclear plates and subsequently treated with 15mM CP for 2-8h or with 2mg/ml cyclohexamide

(CHX) for 1h, or for 2h with a combination of 15mM CP and 2.5mM salubrinal. During the last hour of treatment DMEM was replaced with methionine-free medium. Subsequently, cells were incubated with azide-labeled methionine analogue for 1h and fixed for 15min in 4% formaldehyde and stained according to manufacturer's protocol. DAPI was used as counterstain and images were acquired using a BD-pathway imaging system. Image analysis was performed using BD Attovision software.

FLAG-Co-Immunoprecipitation

U2OS cells, expressing different shRNAs, were transiently transfected with FLAG-tagged wild-type 4EHP or [K121/130/134/222R]-mutant (4KR) 4EHP cDNAs or FLAG-LacR control plasmid in absence or presence of pCAGGS-5HA-mISG15 cDNA in OptiMEM (Invitrogen), using JetPEI (Polyplus Transfection). The following day, medium was refreshed and 48h post transfection cells were lysed in FLAG-lysis buffer (50mM Tris-HCl pH 7.4, 150mM NaCl, 1mM EDTA, 0.5% NP-40, 0.5% Triton-X, 1mM PMSF, supplemented with complete protease inhibitor cocktail (Roche)). After 30 min incubation on ice, lysates were diluted 5 times with FLAG-dilution buffer (50mM Tris-HCl pH 7.4, 150mM NaCl, 1mM EDTA, 1mM PMSF, supplemented with complete protease inhibitor cocktail) and incubated with prewashed M2-FLAG magnetic beads (Sigma) for 3h. Subsequently, beads were washed 3 times for 5min with FLAG-dilution buffer and lysed in Laemmli-SDS-sample buffer. FLAG-ARIH1 co-immunoprecipitation from lysates from SILAC-labeled cells followed by Mass Spectrometry (MS) was performed as described above, with the exception of eluting FLAG-bound proteins by competition with the 3xFLAG peptide instead of boiling in sample buffer. Following elution, samples were trypsinised over-night, desalted, freeze-dried and finally used for MS analysis.

qPCR

RNA was extracted using RNeasy Plus Mini Kit from Qiagen. cDNA was made from 50ng total RNA with RevertAid H minus First strand cDNA synthesis kit (Fermentas) and real-time qPCR was subsequently performed in triplicate using SYBR green PCR (Applied Biosystems) on a 7900HT fast real-time PCR

system (Applied Biosystems). The following qPCR primer sets were used: GAPDH forward (fw) AGCCACATCGCTCAGACACC; GAPDH reverse (rev) ACCCGTTGACTCCGACCTT; ARIH1 fw TCATGCCTCTACCCAAGCCTT; ARIH1 rev ACCAAACCCACAGCAACACA. Data were collected and analysed using SDS2.3 software (Applied Biosystems). Relative mRNA levels after correction for GAPDH control mRNA were expressed using 2^(-ΔΔCt) method.

ACKNOWLEDGEMENTS

We are grateful to Dr. Rob Hoeben, Dr. Dong-Er Zhang, Mr. Martijn Rabelink, and Dr. Klaus Willecke for generously providing cells and reagents. This work was supported by the Netherlands Genomics Initiative /Netherlands Organization for Scientific Research (NWO): nr 050-060-510.

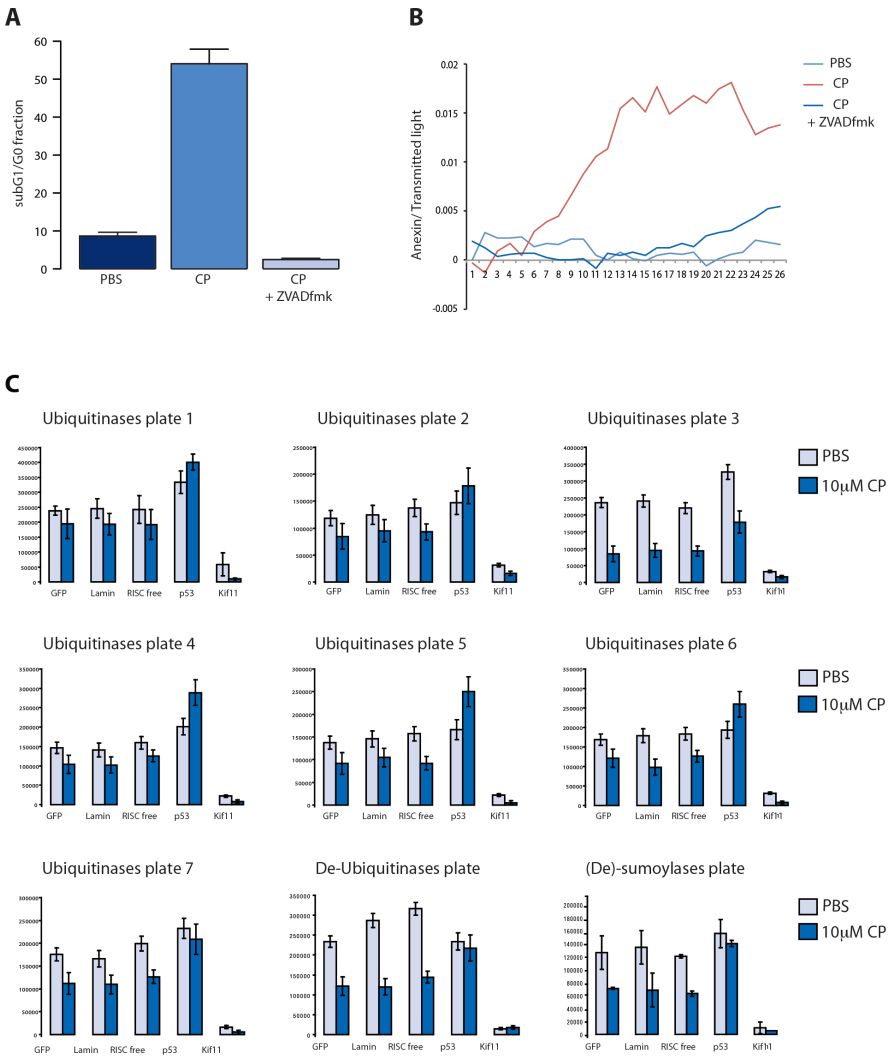

D

$$Z' \text{- factor} = 1 - \frac{3 \times (s_p + s_n)}{|m_p - m_h|} = 0.45$$

Figure S1. Caspase-dependent apoptosis in ES cells treated with CP and quality of ubiquitination/sumoylation screen. (A) Induction of SubG1/G0 apoptotic fraction in HM1 ES cells treated with 7.5μM CP for 24h and prevention by co-treatment with 100μM pan-Caspase inhibitor ZVADfmk. (B) Real time imaging of fluorescently labeled Annexin V binding (Puigvert et al., 2010) shows accumulation of apoptotic ES cells during treatment with 7.5μM CP and prevention by 100μM ZVADfmk. Ratio [AnexinV signal: total cell area] is shown. (C) ATPlite readout for indicated set of control siRNAs in each Smartpool library plate. Bars show average and standard deviation of two control and two 10μM CP-treated plates. (D) Average Z´-factor calculated for siLamin and sip53.

A

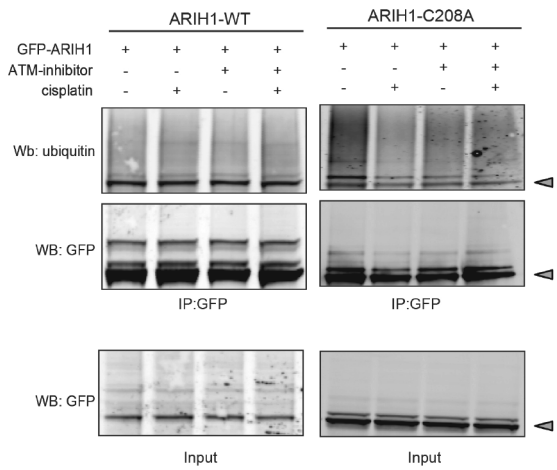

B

IP ARIH1

Protein	Protein name	cPt/untreated
Protein ariadne-1 homolog [Experiment 1]	ARIH1	2,104997264
Ubiquitin-conjugating enzyme E2 L3	UBE2L3/UBCH7 [E2]	1,55649291
Ubiquitin-like modifier-activating enzyme 1	UBA1 [E1]	1,072259573
ubiquitin C;UBC protein;ubiquitin B precursor;ubiquitin and ribosomal protein S27a precursor	Ubiquitin	1,132490006
E3 ubiquitin-protein ligase ARIH1 [Experiment 2]	ARIH1	2,1992039
Ubiquitin-60S ribosomal protein L40;Ubiquitin;60S ribosomal protein L40;Ubiquitin-40S ribosomal protein S27a;Ubiquitin;40S ribosomal protein S27a;Polyubiquitin-B;Ubiquitin;Polyubiquitin-C;Ubiquitin	ubiquitin	1,4406
E3 ubiquitin-protein ligase ARIH1	phospho-ARIH1 Y258	1,0771
Ubiquitin-60S ribosomal protein L40;Ubiquitin;60S ribosomal protein L40;Ubiquitin-40S ribosomal protein S27a;Ubiquitin;40S ribosomal protein S27a;Polyubiquitin-B;Ubiquitin;Polyubiquitin-C;Ubiquitin	K48-ubiquitin	1,5635
E3 ubiquitin-protein ligase ARIH1	ub-ARIH1 K144	0,89212

Figure S2. ARIH1 is part of a ubiquitination complex and CP and ATM inhibitor do not affect ubiquitination of WT or C208A ARIH1. (A) Western blot using antibodies against GFP or ubiquitin on total lysates and GFP-immunoprecipitations from GFP-ARIH1(WT)- and GFP-ARIH(C208A)-expressing U2OS cells treated with vehicle control or treated for 4 hours with 5μM CP with or without pre-treatment for 1hr with 5μM ATM inhibitor KU-55933. Grey arrowheads indicate ARIH1. (B) MS analysis of native FLAG-immunoprecipitations from SILAC-labelled FLAG-ARIH1 U2OS cells. SILAC ratios of peptides detected after 4 hours treatment with 5μM CP and control conditions are shown.

Table S1

Deubiquitinases custom library

Gene Symbol	Gene Id	Accession Number
MJD	110616	NM_029705
E030022H21RIK	217218	NM_001098837
DUB-1A	381944	NM_201409
DUB2	13532	NM_010089
BAP1	104416	NM_027088
C130067A03RIK	320713	NM_177239
TNFAIP3	21929	NM_009397
1810057B09RIK	223527	NM_175009
HIST2H2BE	319190	NM_178214
DXIMX46E	54644	NM_138604
C6.1A	210766	NM_145956
CYLD	74256	NM_173369
FBXO7	69754	NM_153195
FBXO8	50753	NM_015791
E130307M08RIK	68047	NM_026530
1300006C06RIK	74158	NM_028792
1110007C05RIK	66124	NM_025368
OTUB1	107260	NM_134150
4930586I02RIK	68149	NM_026580
4933428L19RIK	71198	XM_991213
D8ERTD69E	73945	NM_001081164
2600013N14RIK	72201	NM_152812
USP1	230484	NM_146144
USP2	53376	NM_198091
USP3	235441	NM_144937
USP4	22258	NM_011678
USP5	22225	NM_013700
USP7	252870	NM_001003918
USP8	84092	NM_019729
USP9X	22284	NM_009481
USP9Y	107868	NM_148943
USP10	22224	NM_009462
USP11	236733	NM_145628
USP12	22217	NM_011669
USP13	72607	NM_001013024
USP14	59025	NM_001038589
USP15	14479	NM_027604
USP16	74112	NM_024258
Usp17	436004	NM_001033494
USP18	24110	NM_011909
USP19	71472	NM_027804
USP20	74270	NM_028846
USP21	30941	NM_013919
USP22	216825	NM_001004143
Usp24	329908	XM_915524
USP25	30940	NM_013918
USP26	83563	NM_031388
USP28	235323	NM_175482
USP29	57775	NM_021323
USP30	100756	NM_001033202
6330567E21RIK	76179	XM_992065
USP32	237898	NM_001029934

Table S1. Custom siRNA libraries for Deubiquitinases and (De)-Sumoylases. Indicated are gene symbols, Entrez IDs and Accession numbers.

USP33	170822	NM_001076676
LOC244144	244144	XM_886523
Usp36	72344	XM_916680
4932415L06RIK	319651	NM_176972
USP38	74841	NM_027554
USP39	28035	NM_138592
USP40	227334	NM_001033291
Usp42	76800	NM_029749
USP43	216835	NM_173754
E430004F17	327799	NM_183199
4930550B20RIK	77593	NM_152825
2410018I08RIK	69727	NM_177561
USP47	74996	NM_133758
USP48	170707	NM_130879
C330046L10RIK	224836	NM_198421
4930511O11RIK	75083	NM_029163
LOC635253	635253	NM_001137547
USP52	103135	NM_133992
AA939927	99526	NM_133857
USP54	78787	NM_030180
UBR1	22222	NM_009461
UCHL1	22223	NM_011670
UCHL3	50933	NM_016723
UCHL5	56207	NM_019562
UFD1L	22230	NM_011672
UBE4B	63958	NM_022022
COPS5	26754	NM_013715
PLP2	18824	NM_019755

SUMOylation custom library

Gene Symbol	Gene Id	Accession Number
UBLE1B	50995	NM_016682
Ube2i	22196	NM_011665
MDM2	17246	NM_010786
D11BWG0280E	52915	NM_028601
BC065120	328365	NM_183208
PIAS1	56469	NM_019663
MIZ1	17344	NM_008602
PIAS3	229615	NM_018812
PIAS4	59004	NM_021501
RANBP2	19386	NM_011240
CBX4	12418	NM_007625
2510027N19RIK	67711	NM_026330
TOPORS	106021	NM_134097
RNF110	22658	NM_009545
SENP1	223870	NM_144851
SENP2	75826	NM_029457
SENP3	80886	NM_030702
SENP5	320213	NM_177103
SENP6	215351	NM_146003
2810413I22RIK	66315	NM_001003973
SENP8	71599	NM_027838

Table S1 (continued). Custom siRNA libraries for Deubiquitinases and (De)-Sumoylases. Indicated are gene symbols, Entrez IDs and Accession numbers.

Table S2.

gene symbol	Z-score	p-value
RBX1	-3.49229	0.000239
FBXO6A	-2.96913	0.001493
SYTL4	-2.69639	0.003505
RCHY1	-2.68571	0.003619
RNF166	-2.67699	0.003714
Rfwd3	-2.51751	0.005909
UBE1X	-2.28613	0.011123
TCE1	-2.25446	0.012084
ARIH1	-2.16801	0.015079
FBXW7	-2.11149	0.017365
TOPORS	-2.11004	0.017428
BARD1	-2.05953	0.019722
C730024G19RIK	-2.05522	0.019929
LOC380928	-2.0437	0.020492
LOC381621	-2.02454	0.021458
USP8	-2.02454	0.021458
UBE2D3	-2.02396	0.021487
CHD4	-1.93042	0.026778
BRCA1	-1.85984	0.031454
PHF15	-1.85	0.032157
TRIM21	-1.80426	0.035595
SHPRH	-1.75546	0.03959
MKRN2	-1.73969	0.040957
USP4	-1.73969	0.040957
A530081L18RIK	-1.70491	0.044106
DXIMX46E	-1.70491	0.044106
FBXW5	-1.68291	0.046196
USP5	-1.45575	0.07273
USP7	-1.37068	0.085238
Usp42	1.637496	0.050763
FBXO17	1.650206	0.04945
ASB3	1.656369	0.048824
1110002E23RIK	1.708269	0.043793
LOC668173	1.728961	0.041908
6330567E21RIK	1.728961	0.041908
Trim61	1.750478	0.040018
FBXO34L	1.804707	0.03556
MGRN1	1.934613	0.026519
4933428L19RIK	1.934613	0.026519
DTX2	1.986825	0.023471
AL033326	2.010687	0.022179
USP54	2.078665	0.018824
ZNRF2	2.153452	0.015642
LNX2	2.196345	0.014034
CUL4A	2.21634	0.013334
RNF110	2.29063	0.010992
USP22	2.29063	0.010992
CUL1	2.479363	0.006581
CDC34	2.994131	0.001376
E430004F17	3.097247	0.000977

Table S2. Hits from primary screens. Indicated are gene symbols, Z-scores and p-values.

Table S3.

	gene ID	Accession number	Function	validation
USP4 *	22258	NM_011678	**DUB**	**2 out of 4**
USP7 *	252870	NM_001003918	**DUB**	**3 out of 4**
USP8	84092	NM_019729	**DUB**	**4 out of 4**
DXIMX46E	54644	NM_138604	**DUB**	**2 out of 4**
E430004F17	327799	NM_183199	**DUB**	**2 out of 4**
USP5 *	22225	NM_013700	**DUB**	**3 out of 4**
RUFY1	216724	NM_172557	**no known UB-function**	**2 out of 4**
RCHY1 *	68098	NM_026557	**E3**	**2 out of 4**
Rfwd3 *	234736	NM_146218	**E3**	**4 out of 4**
4930470D19RIK	67610	NM_026274	**no known UB-function**	**4 out of 4**
ARIH1	23806	NM_019927	**E3**	**4 out of 4**
UBE1X	22201	NM_009457	**E1**	**4 out of 4**
SYTL4	94121	NM_013757	**no known UB-function**	**3 out of 4**
CHD4	107932	NM_145979	**no known UB-function**	**3 out of 4**
FBXW7	50754	NM_080428	**E3**	**2 out of 4**
LOC381621		XM_355579	**no known UB-function**	**2 out of 4**
UBE2D3	66105	NM_025356	**E2**	**4 out of 4**
DTX2	74198	NM_023742	**E3**	**2 out of 4**
ZNRF2	387524	NM_199143	**E3**	**2 out of 4**
RBX1	9978	NM_019712	**E3**	**4 out of 4**
TCE1	79043	NM_027141	**no known UB-function**	**2 out of 4**
TOPORS *	106021	NM_134097	**E3**	**2 out of 4**
C730024G19RIK	232566	XM_132975	**no known UB-function**	**3 out of 4**
BRCA1	NM_009764	NM_009764	**E3**	**3 out of 4**
TRIM21	20821	NM_009277	**E3**	**4 out of 4**
SHPRH	268281	NM_172937	**E3**	**2 out of 4**
AL033326*	24105	NM_019705	**E3**	**3 out of 4**
Fbxo7	**69754**	**NM_153195**	**E3**	**3 out of 4**

Table S3. Hits from secondary deconvolution screens. Indicated are gene symbols, Entrez IDs, Accession numbers, ubiquitination function and validation status. Asterisks indicate hits known to affect p53. Sensitising siRNAs in blue; protecting siRNAs in red.

REFERENCES

1. Ciccia, A. and S.J. Elledge, The DNA damage response: making it safe to play with knives. Mol Cell, 2010. 40(2): p. 179-204.

2. Jackson, S.P. and J. Bartek, The DNA-damage response in human biology and disease. Nature, 2009. 461(7267): p. 1071-8.

3. Matsuoka, S., et al., ATM and ATR substrate analysis reveals extensive protein networks responsive to DNA damage. Science, 2007. 316(5828): p. 1160-6.

4. Reinhardt, H.C. and M.B. Yaffe, Kinases that control the cell cycle in response to DNA damage: Chk1, Chk2, and MK2. Curr Opin Cell Biol, 2009. 21(2): p. 245-55.

5. Bergink, S. and S. Jentsch, Principles of ubiquitin and SUMO modifications in DNA repair. Nature, 2009. 458(7237): p. 461-7.

6. Komander, D., The emerging complexity of protein ubiquitination. Biochem Soc Trans, 2009. 37(Pt 5): p. 937-53.

7. Morris, J.R., More modifiers move on DNA damage. Cancer Research, 2010. 70(10): p. 3861-3.

8. Skaug, B. and Z.J. Chen, Emerging role of ISG15 in antiviral immunity. Cell, 2010. 143(2): p. 187-90.

9. Staub, O., Ubiquitylation and isgylation: overlapping enzymatic cascades do the job. Sci STKE, 2004. 2004(245): p. pe43.

10. Brooks, C.L. and W. Gu, p53 ubiquitination: Mdm2 and beyond. Mol Cell, 2006. 21(3): p. 307-15.

11. Crosetto, N., M. Bienko, and I. Dikic, Ubiquitin hubs in oncogenic networks. Mol Cancer Res, 2006. 4(12): p. 899-904.

12. Wood, L.M., et al., A novel role for ATM in regulating proteasome-mediated protein degradation through suppression of the ISG15 conjugation pathway. PLoS One, 2011. 6(1): p. e16422.

13. Kerscher, O., R. Felberbaum, and M. Hochstrasser, Modification of proteins by ubiquitin and ubiquitin-like proteins. Annu Rev Cell Dev Biol, 2006. 22: p. 159-80.

14. Nagy, V. and I. Dikic, Ubiquitin ligase complexes: from substrate selectivity to conjugational specificity. Biol Chem, 2010. 391(2-3): p. 163-9.

15. Wenzel, D.M., et al., UBCH7 reactivity profile reveals parkin and HHARI to be RING/HECT hybrids. Nature, 2011. 474(7349): p. 105-8.

16. Reinhardt, H.C., et al., Is post-transcriptional stabilization, splicing and translation of selective mRNAs a key to the DNA damage response? Cell Cycle, 2011. 10(1):

p. 23-7.

17. Braunstein, S., et al., Regulation of protein synthesis by ionizing radiation. Molecular and Cellular Biology, 2009. 29(21): p. 5645-56.

18. Connolly, E., et al., Hypoxia inhibits protein synthesis through a 4E-BP1 and elongation factor 2 kinase pathway controlled by mTOR and uncoupled in breast cancer cells. Molecular and Cellular Biology, 2006. 26(10): p. 3955-65.

19. Silvera, D., S.C. Formenti, and R.J. Schneider, Translational control in cancer. Nat Rev Cancer, 2010. 10(4): p. 254-66.

20. Kong, J. and P. Lasko, Translational control in cellular and developmental processes. Nat Rev Genet, 2012. 13(6): p. 383-94.

21. Gross, J.D., et al., Ribosome loading onto the mRNA cap is driven by conformational coupling between eIF4G and eIF4E. Cell, 2003. 115(6): p. 739-50.

22. Gingras, A.C., B. Raught, and N. Sonenberg, eIF4 initiation factors: effectors of mRNA recruitment to ribosomes and regulators of translation. Annu Rev Biochem, 1999. 68: p. 913-63.

23. Moudry, P., et al., Ubiquitin-activating enzyme UBA1 is required for cellular response to DNA damage. Cell Cycle, 2012. 11(8): p. 1573-82.

24. Puigvert, J.C., et al., Systems Biology Approach Identifies the Kinase Csnk1a1 as a Regulator of the DNA Damage Response in Embryonic Stem Cells. Sci Signal, 2013. 6(259).

25. Dayal, S., et al., Suppression of the deubiquitinating enzyme USP5 causes the accumulation of unanchored polyubiquitin and the activation of p53. J Biol Chem, 2009. 284(8): p. 5030-41.

26. Meulmeester, E., et al., Loss of HAUSP-mediated deubiquitination contributes to DNA damage-induced destabilization of Hdmx and Hdm2. Mol Cell, 2005. 18(5): p. 565-76.

27. Zhang, X., et al., USP4 inhibits p53 through deubiquitinating and stabilizing ARF-BP1. EMBO J, 2011. 30(11): p. 2177-89.

28. Fu, X., et al., RFWD3-Mdm2 ubiquitin ligase complex positively regulates p53 stability in response to DNA damage. Proc Natl Acad Sci U S A, 2010. 107(10): p. 4579-84.

29. Yang, X., et al., Plk1-mediated phosphorylation of Topors regulates p53 stability. J Biol Chem, 2009. 284(28): p. 18588-92.

30. Lin, J.R., et al., SHPRH and HLTF act in a damage-specific manner to coordinate different forms of postreplication repair and prevent mutagenesis. Mol Cell, 2011. 42(2): p. 237-49.

31. Jung, Y.S., et al., Pirh2 E3 ubiquitin ligase monoubiquitinates DNA polymerase eta to suppress translesion DNA synthesis. Molecular and Cellular Biology, 2011.

31(19): p. 3997-4006.

32. Roy, R., J. Chun, and S.N. Powell, BRCA1 and BRCA2: different roles in a common pathway of genome protection. Nat Rev Cancer, 2012. 12(1): p. 68-78.

33. Liu, S., et al., RING finger and WD repeat domain 3 (RFWD3) associates with replication protein A (RPA) and facilitates RPA-mediated DNA damage response. J Biol Chem, 2011. 286(25): p. 22314-22.

34. Tan, N.G.S., et al., Characterisation of the human and mouse orthologues of the Drosophila ariadne gene. Cytogenetics and Cell Genetics, 2000. 90(3-4): p. 242-245.

35. Li, Z., P.R. Musich, and Y. Zou, Differential DNA damage responses in p53 proficient and deficient cells: cisplatin-induced nuclear import of XPA is independent of ATR checkpoint in p53-deficient lung cancer cells. Int J Biochem Mol Biol, 2011. 2(2): p. 138-145.

36. Medema, R.H. and L. Macurek, Checkpoint control and cancer. Oncogene, 2012. 31(21): p. 2601-13.

37. Kumar, V., et al., Regulation of the rapamycin and FKBP-target 1/mammalian target of rapamycin and cap-dependent initiation of translation by the c-Abl protein-tyrosine kinase. J Biol Chem, 2000. 275(15): p. 10779-87.

38. Tan, N.G., et al., Human homologue of ariadne promotes the ubiquitylation of translation initiation factor 4E homologous protein, 4EHP. FEBS Lett, 2003. 554(3): p. 501-4.

39. Okumura, F., W. Zou, and D.E. Zhang, ISG15 modification of the eIF4E cognate 4EHP enhances cap structure-binding activity of 4EHP. Genes Dev, 2007. 21(3): p. 255-60.

40. Ardley, H.C., et al., Features of the parkin/ariadne-like ubiquitin ligase, HHARI, that regulate its interaction with the ubiquitin-conjugating enzyme, Ubch7. J Biol Chem, 2001. 276(22): p. 19640-7.

41. Matsumoto, A., et al., Fbxw7-dependent degradation of Notch is required for control of „stemness“ and neuronal-glial differentiation in neural stem cells. J Biol Chem, 2011. 286(15): p. 13754-64.

42. Welcker, M. and B.E. Clurman, FBW7 ubiquitin ligase: a tumour suppressor at the crossroads of cell division, growth and differentiation. Nat Rev Cancer, 2008. 8(2): p. 83-93.

43. Yi, Z., T. Yi, and Z. Wu, cDNA cloning, characterization and expression analysis of DTX2, a human WWE and RING-finger gene, in human embryos. DNA Seq, 2006. 17(3): p. 175-80.

44. Balut, C.M., C.M. Loch, and D.C. Devor, Role of ubiquitylation and USP8-dependent deubiquitylation in the endocytosis and lysosomal targeting of plasma membrane KCa3.1. Faseb Journal, 2011. 25(11): p. 3938-48.

45. Kuroda, T.S., et al., The Slp homology domain of synaptotagmin-like proteins 1-4 and Slac2 functions as a novel Rab27A binding domain. J Biol Chem, 2002. 277(11): p. 9212-8.

46. Yamamoto, H., et al., Functional cross-talk between Rab14 and Rab4 through a dual effector, RUFY1/Rabip4. Molecular Biology of the Cell, 2010. 21(15): p. 2746-55.

47. Larsen, D.H., et al., The chromatin-remodeling factor CHD4 coordinates signaling and repair after DNA damage. Journal of Cell Biology, 2010. 190(5): p. 731-40.

48. Nakayama, E.E. and T. Shioda, Anti-retroviral activity of TRIM5 alpha. Rev Med Virol, 2010. 20(2): p. 77-92.

49. Okumura, F., et al., The Role of Elongin BC-Containing Ubiquitin Ligases. Front Oncol, 2012. 2: p. 10.

50. Cencic, R., et al., Reversing chemoresistance by small molecule inhibition of the translation initiation complex eIF4F. Proc Natl Acad Sci U S A, 2011. 108(3): p. 1046-51.

51. Shamji, A.F., P. Nghiem, and S.L. Schreiber, Integration of growth factor and nutrient signaling: implications for cancer biology. Mol Cell, 2003. 12(2): p. 271-80.

52. Clarke, R., et al., Endoplasmic reticulum stress, the unfolded protein response, autophagy, and the integrated regulation of breast cancer cell fate. Cancer Research, 2012. 72(6): p. 1321-31.

53. Morita, M., et al., A novel 4EHP-GIGYF2 translational repressor complex is essential for mammalian development. Molecular and Cellular Biology, 2012. 32(17): p. 3585-93.

54. Sonenberg, N. and A.C. Gingras, The mRNA 5‘ cap-binding protein eIF4E and control of cell growth. Curr Opin Cell Biol, 1998. 10(2): p. 268-75.

55. Cho, P.F., et al., A new paradigm for translational control: inhibition via 5‘-3‘ mRNA tethering by Bicoid and the eIF4E cognate 4EHP. Cell, 2005. 121(3): p. 411-23.

56. Lasko, P., Posttranscriptional regulation in Drosophila oocytes and early embryos. Wiley Interdiscip Rev RNA, 2011. 2(3): p. 408-16.

57. Bensimon, A., et al., ATM-dependent and -independent dynamics of the nuclear phosphoproteome after DNA damage. Sci Signal, 2010. 3(151): p. rs3.

58. Bennetzen, M.V., et al., Site-specific phosphorylation dynamics of the nuclear proteome during the DNA damage response. Mol Cell Proteomics, 2010. 9(6): p. 1314-23.

59. Joshi, B., A. Cameron, and R. Jagus, Characterization of mammalian eIF4E-family members. Eur J Biochem, 2004. 271(11): p. 2189-203.

60. Wiseman, R.L. and W.E. Balch, A new pharmacology--drugging stressed folding pathways. Trends Mol Med, 2005. 11(8): p. 347-50.

61. Campeau, E., et al., A versatile viral system for expression and depletion of proteins in mammalian cells. PLoS One, 2009. 4(8): p. e6529.

62. Birmingham, A., et al., Statistical methods for analysis of high-throughput RNA interference screens. Nat Methods, 2009. 6(8): p. 569-75.

63. Puigvert, J.C., et al., High-throughput live cell imaging of apoptosis. Curr Protoc Cell Biol, 2010. Chapter 18: p. Unit 18 10 1-13.

64. Moody, C.A., et al., Modulation of the cell growth regulator mTOR by Epstein-Barr virus-encoded LMP2A. Journal of Virology, 2005. 79(9): p. 5499-506.